CHAPTER 5

ROLE OF POINT DEFECTS ON THE ENHANCEMENT OF FERROMAGNETISM IN ZnO NRs

This chapter discusses the enhancement of ferromagnetism in undoped ZnO NRs. At first, the vertically aligned ZnO NRs have been grown on silicon substrates without any external catalyst by RF magnetron sputtering technique. The role of point defects on the ferromagnetic behavior of ZnO NRs is analyzed by subjecting the as-grown ZnO NRs to post growth treatment under oxygen and vacuum atmospheres which significantly suppresses the point defects. Consequently, the decrease of ferromagnetism in post annealed ZnO NRs is observed, that is directly associated with the compensation of point defects.

5.1 Introduction

The theoretical prediction of room temperature ferromagnetism in DMS materials has triggered a considerable interest in the field of spintronics, which could pave the way to use spin in addition to charge in semiconductor devices [100]. In continuation, many research groups have paid their considerable attention on DMS materials and proved experimentally that can exhibit RTFM [101]. Although the origin of ferromagnetism in oxide DMS materials is still not clear, the segregation of magnetic clusters is believed to explain the ferromagnetic behavior of oxide semiconductors [102]. The magnetic properties of the oxide semiconductors are not only related to the existence of the transition metal (TM) ions but also depend on the defects in the semiconductors. Hence, the growth conditions and post growth treatments play an important role in ferromagnetic nature of the materials since they can create point defects in oxide semiconductors which are similar to carrier doping. Thus, the defects could introduce RTFM in the non-magnetic semiconductors [103].

The observation of ferromagnetism in TM doped ZnO at and above room temperature makes it a potential candidate in the field of spintronics. The origin

of ferromagnetism in TM doped ZnO is due to the significance of the point defects as well as the secondary phases, which lead to the ferromagnetic ordering of the materials and increase the Curie temperature (T_c). On the other hand, the ferromagnetic behavior of undoped ZnO solely depends on the point defects such as oxygen vacancies (V_o), oxygen interstitials (O_i), Zn vacancies (V_{Zn}) and Zn interstitials (Zn_i) [104-107]. In this chapter, we report the growth of well aligned ZnO NRs on the silicon (111) substrates by RF magnetron sputtering without any external catalyst. The structural, optical and magnetic properties of ZnO NRs are described and the role of point defects on the origin of the ferromagnetism and their exchange interactions are discussed on the basis of the optical transitions.

5.2 Experimental procedure

Vertically aligned ZnO NRs have been fabricated on Si(111) substrates at elevated temperature by RF magnetron sputtering. In brief, the chamber was evacuated to the base pressure of 5 x 10^{-6} mbar and the deposition was carried out under pure Ar atmosphere at the pressure of 6 x 10^{-3} mbar. The target to substrate distance was kept constant at 50 mm and the deposition was performed for 60 min at 550 °C with the rf power of 140 W. To understand the role of impurities which induce or annihilate the magnetic interactions in 1-D NSs, the as-grown (AG) NRs are subjected to annealing process at 500 °C for 30 min under oxygen (0.1 mbar) and vacuum (1 x 10^{-5} mbar) environment.

5.3 Results and discussion

Fig. 5.1 (a) depicts the XRD spectra of as-grown (AG), vacuum annealed (VA) and oxygen annealed (OA) ZnO NRs. All the peaks are indexed according to the wurtzite hexagonal structure of ZnO. The relatively dominant (002) reflection of the ZnO NRs implies that most of the NRs are aligned vertically along the c-axis. The presence of weak (103) reflection depicts that significantly feeble number of ZnO NRs are aligned in this direction. This illustrates that the quasi alignment of NRs along the c-axis. In addition to this, a weak reflection around at 64.5° corresponds to the SiO_2 (JCPDS Card No. 89-3607). It provides

an evidence for the presence of SiO_2 layer on the top surface of the silicon substrate, which may be formed due to the oxidation of the silicon during the early stage of growth and followed by post growth process. The (002) peak position of the AG ZnO NRs (34.39°) is less than the bulk value (34.45°), indicating that the NRs are in the state of uniform compressive strain [108]. It is worth noted that the (002) peak position of the VA and OA NRs shifts about 0.02° linearly towards its bulk value as shown in Fig. 5.1 (b). This provides an evidence for the relaxation of the compressive strain due to the post growth treatment. The compressive strain in the AG NRs has its origin in the imperfection of the crystallites during growth [109].

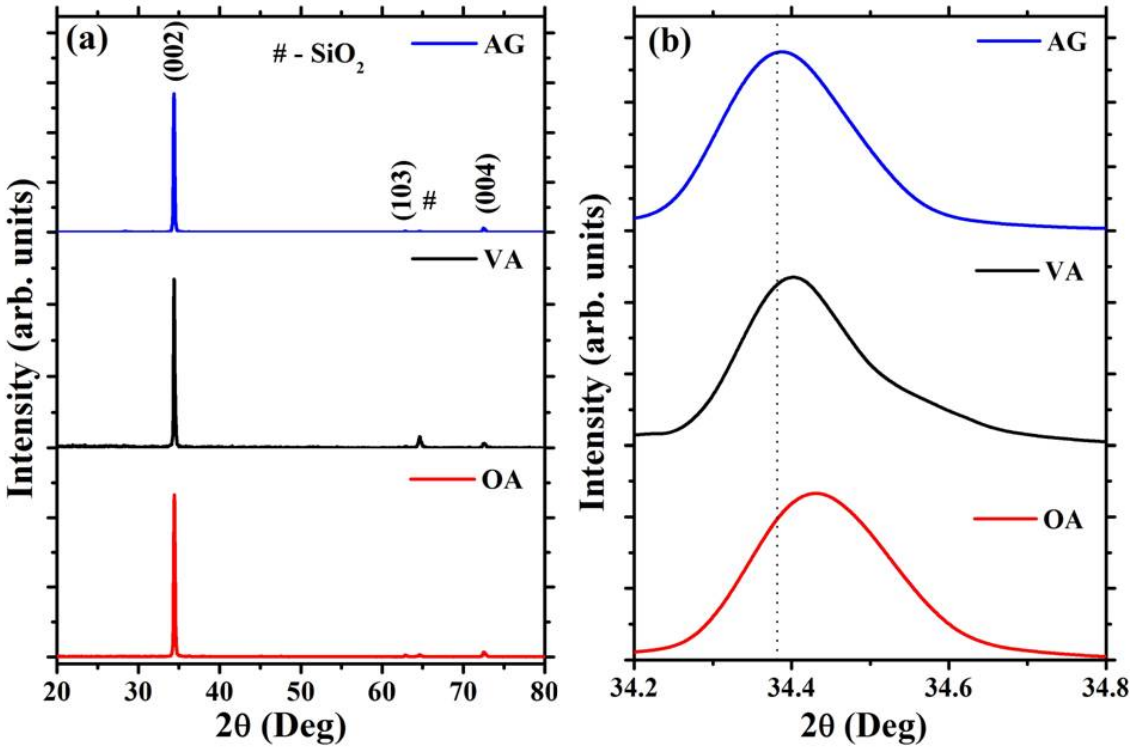

Fig. 5.1 (a) Typical X – ray diffraction pattern of vertically aligned undoped ZnO NRs on Silicon (111) substrate and (b) (002) peak position of AG, VA and OA undoped ZnO NRs.

Figs. 5.2 (a) & (b) show the FESEM images of the ZnO NRs grown on silicon (111) substrates. These images confirm that NRs are well aligned normal to the substrate with smooth surfaces and nearly uniform diameter along the

axial direction. The FESEM images also reveal the hexagonal cross section of the ZnO NRs along the c- axis. The average length and diameter of the ZnO NRs are ~1.5 μm and ~350 nm respectively.

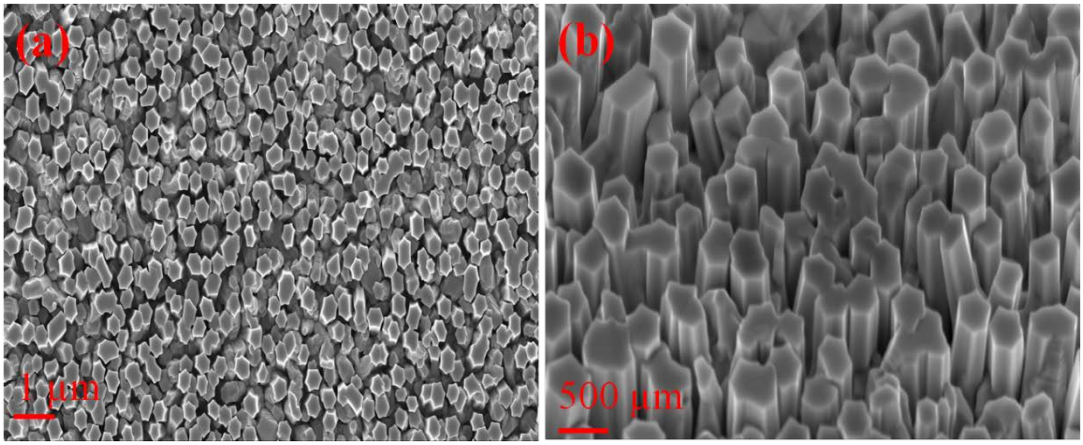

Fig. 5.2 FESEM images of AG undoped ZnO NRs. (a) top view and (b) 60 ° tilted view.

Fig. 5.3 shows the room temperature micro-Raman spectra of the ZnO NRs, grown under identical conditions and subordinated to various post growth treatments. A sharp peak at 99.7 cm^{-1} corresponds to the E_2^{low} phonon mode of ZnO, which is attributed to the lattice vibrations of zinc atoms. E_2^{high} phonon mode is typically used to describe the strain, crystalline nature and phase orientation. It is well known that the E_2^{high} phonon mode at 437 cm^{-1} is used to characterize the strain in ZnO lattice; these vibrations are related to the lattice vibration of the oxygen atoms and indicating the wurtzite phase of ZnO [85]. The Lorentz fitted E_2^{high} mode at 438.9 cm^{-1} of the AG ZnO NRs was blue shifted about 1.9 cm^{-1} from its standard value. The shift in E_2^{high} phonon mode describes that the AG ZnO NRs are under compressive strain [65]. E_2^{high} peak of VA and OA ZnO NRs was observed at 438.6 cm^{-1} and 438.3 cm^{-1} respectively which are red shifted as compared to the AG NRs. It demonstrates that the compressive strain in the AG ZnO NRs was partially relaxed due to the post growth treatment under vacuum and oxygen atmospheres. The variation of E_2^{high}

peak position and FWHM is shown in Table 5.1. The additional Raman modes at around 302, 520, 620 and 670 cm^{-1} correspond to the optic and acoustic modes of the silicon substrate respectively [71].

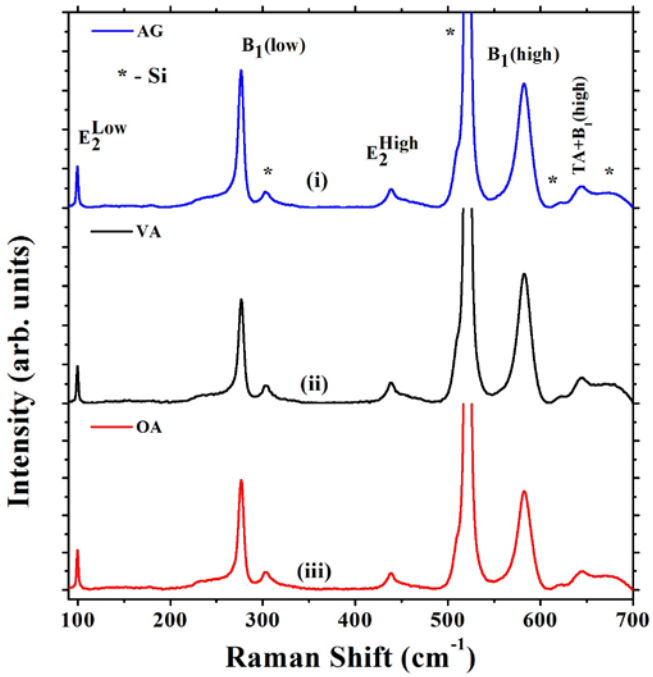

Fig. 5.3 Room temperature Raman spectra of vertically aligned AG and post-annealed undoped ZnO NRs recorded in the back-scattering geometry. (i) As-Grown (AG), (ii) Vacuum Annealed (VA) and (iii) Oxygen Annealed (OA).

The peak at 582 cm^{-1} can be attributed to either E_1(LO) or B_1(high) mode. However, it is reported that E_1(LO) mode observed at 581 cm^{-1} arises due to the oxygen deficiency such as oxygen vacancies [68]. In our case, the oxygen vacancies are present only in AG ZnO NRs and it is compensated by the post growth treatments as explained in PL measurements. The position and intensity of the peak at 582 cm^{-1} remain the same for the all samples. Hence, it could not be assigned to E_1(LO). Due to the small dispersion along the Brillouin zone, the observed peaks at 276 and 582 cm^{-1} can be attributed to silent modes [B_1(low) & B_1(high)] of ZnO [110]. Further, the B_1(low) mode is located near to the region of low two phonon density of states while the B_1(high) mode is near to the

region of high two phonon density of states. Hence, we observed that both B_1(low) and B_1(high) modes exhibit comparable intensities and the width of B_1(low) mode is one third of the width of B_1(high) [66].

Table 5.1. E_2^{high} peak position and FWHM of the AG and post-annealed ZnO NRs.

Sample	E_2^{high} (cm^{-1})	FWHM (cm^{-1})
AG	438.9	13.06
VA	438.6	12.69
OA	438.3	12.42

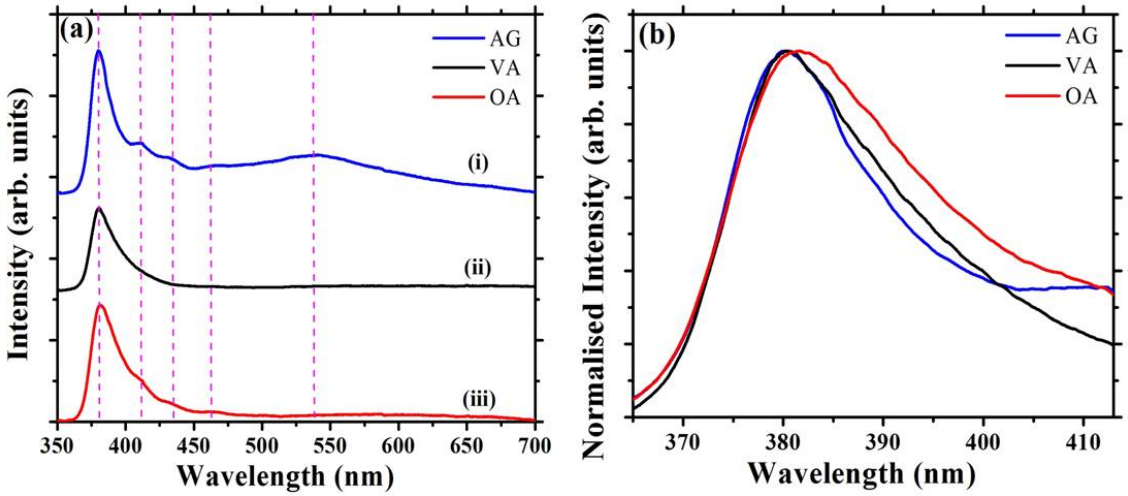

Fig. 5.4 (a) RTPL spectra of AG and post-annealed undoped ZnO NRs. (i) As-Grown (AG), (ii) Vacuum Annealed (VA) and (iii) Oxygen Annealed (OA) and (b) Enlarged view of the near band edge (NBE) emission of the PL spectra.

Fig. 5.4 (a) shows the room temperature photoluminescence (RTPL) spectra of the ZnO NRs grown under identical conditions, but subjected to different post growth treatments under oxygen and vacuum atmospheres. PL spectrum of AG ZnO NRs shows the UV (380 nm), violet (410 nm), blue (430 &

465 nm) and green (541 nm) emissions. The visible region of the PL spectra clearly illustrates the existence of point defects both in AG and OA ZnO NRs. However, the green luminescence is absolutely suppressed in OA NRs at 500 °C due to the passivation of oxygen vacancy induced point defects. Nevertheless, the violet and blue transitions can be related to the point defects of zinc such as zinc vacancy and interstitial zinc [88]. On the other hand, all the visible emissions are completely suppressed in the VA NRs due to the recrystallization process. The surface adsorbed oxygen atoms are expected to diffuse into the oxygen vacancy site during the post growth process. The surface adsorbed oxygen atoms do not leave the surface as O_2 molecules and it is energetically less stable than ZnO lattice. Hence, the oxygen vacancies are likely to be compensated by the surface adsorbed oxygen atoms through diffusion. The UV emission peak of VA and OA ZnO NRs is slightly red shifted as compared to the AG ZnO NRs. This shows the presence of small residual compressive strain in the AG NRs and the strain was partially relaxed during the post growth treatments at high temperature, as evidenced by the red shift in the band gap of the ZnO NRs [111] and it is clearly shown in the Fig. 5.4 (b). These results corroborate with the XRD and Raman data and confirm the existence of compressive strain.

Zinc vacancy (V_{Zn}) will act as an acceptor and create an acceptor level above the valence band. It was accounted that the energy difference between the conduction band minimum and the zinc vacancy level (V_{Zn}) is about 3.06 eV [74]. This shows that the acceptor level is well above the valence band about 0.3 eV. We believe that the observed peak at 410 nm is the electron transition from the conduction band to the V_{Zn} level and this transition provides a clear evidence for the presence of zinc vacancy in the ZnO NRs. Interstitial zinc (Zn_i) produces the shallow and deep level donors at 0.5 and 1.3 eV below the bottom of the conduction band. In the emission spectra, the peak at 430 nm is assigned to the recombination of an electron from the shallow level donor of Zn_i to a hole in the

valence band [75]. The blue emission at 465 nm corresponds to the transition electron from the conduction band to the singly ionized zinc vacancy (V_{Zn}^{-}), which lies around 2.66 eV below the conduction band. A broad peak around 541 nm corresponds to oxygen vacancies and this green luminescence is attributed to the electron transition from the shallow donor level (V_o) to a shallow acceptor level (V_{Zn}) [76]. These transitions confirm the existence of the oxygen and zinc vacancies in the AG ZnO NRs. In the OA NRs, the intensity of green luminescence is substantially suppressed which means that the oxygen vacancies are totally counterbalanced and the intensity of the blue luminescence is reduced considerably by the partial compensation of zinc vacancies. Hence, the only possible emission for the blue luminescence is the transition between conduction band and acceptor level. In the VA NRs, the intensities of blue and green luminescence are totally suppressed by the consequence of the compensation of zinc and oxygen vacancies. Hence, the defect mediated emissions are absent and only near band edge emission is present in the VA NRs.

Fig. 5.5 (a) shows the temperature dependent magnetization curves of AG and post annealed ZnO NRs recorded at constant field strength of 1000 Oe. The temperature dependent magnetization is recorded by performing zero field cooled (ZFC) and field cooled (FC) magnetization measurements at the temperature range of 2-300 K. In the entire temperature range, ZFC and FC curves do not show any transition from ferromagnetic to paramagnetic phase, which reveals that the Curie temperature of the undoped ZnO NRs is well above the room temperature (300 K). At low temperature around 7 K, there is a clear cusp in both ZFC and FC temperature dependent magnetization curves, which indicates a spin-glass behavior [112]. This spin glass behavior correlates the coexistence of ferromagnetic and anti-ferromagnetic interaction. However, the ferromagnetic phase is still strongly dominant and stable over the whole range of temperatures (2-300 K). At low temperature (2 K), the value of coercivity is large as compared to room temperature and it provides a strong evidence for the

existence of ferromagnetism along with a small anti-ferromagnetic nature of ZnO NRs.

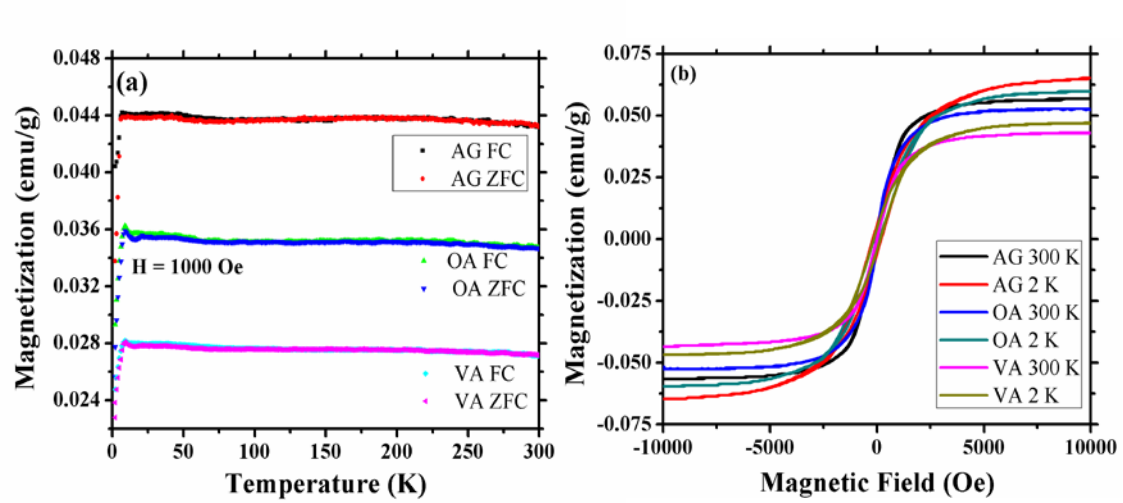

Fig. 5.5 (a) Temperature dependent ZFC and FC magnetization curves recorded under constant field of 1 kOe for ZnO NRs and (b) Magnetic hysteresis loops of the undoped ZnO NRs (as-grown and post-annealed (OA and VA)) at 2 and 300 K.

The magnetization versus magnetic field (M-H) curves of AG and post annealed (both oxygen and vacuum at 500 °C) ZnO NRs is shown in Fig. 5.5 (b). The hysteresis loops along ZFC and FC clearly indicate that NRs have undisputable RTFM. The actual magnetization of AG and post annealed NRs is determined by subtracting the diamagnetic contribution of the silicon substrate from the raw data. The unit of magnetization is converted into emu/g by considering the diameter, length and density with hexagonal geometry of the NRs.

ZFC and FC curves of AG NRs show very high stable FM and can be related to the presence of oxygen and zinc vacancies as revealed by PL transitions in visible region. On the other hand, the magnetization is considerably decreased due to the compensation of oxygen vacancies as the NRs were annealed under oxygen atmosphere and however zinc vacancies remain as evidence by the blue luminescence at 410 nm. Nevertheless, the complete suppression of point defects in VA NRs gives rise to the softening of RTFM but

it unable to vanish the ferromagnetism as opposed to the absence of vacancies induced blue and green emissions. The presence of RTFM in VA samples where no vacancies of oxygen and zinc are observed by PL transitions envisage that vacancies induced point defects alone not solely responsible for the magnetic moment in undoped ZnO NRs. Thus, one can conclude that the intrinsic defects and surface related impurity transitions are expected greatly to be responsible for the origin of FM in ZnO NRs. As expected, the defect induced ferromagnetism would be decreased by the improvement of the crystalline nature through annealing processes. The magnetization decreases considerably after annealing both in oxygen and vacuum at 500 °C for 30 min. The saturation magnetization and coercivity of ZnO NRs are shown in Table 5.2. The coercivity is enhanced at lower temperature (i.e., 2K) as compared to the room temperature (i.e., 300K) in the ZnO NRs. This is called as broadening effect which is a classical behavior of the magnetic materials at low temperature. The origin of the RTFM in pure ZnO NRs may be attributed to the exchange interactions between unpaired electron spins arising from either vacancies or surface defects [113].

Table 5.2. Magnetization and Coercivity of the AG and post-annealed ZnO NRs.

Parameters	**As-grown**		**Oxygen annealed**		**Vacuum annealed**	
	2K	**300K**	**2K**	**300K**	**2K**	**300K**
Saturation magnetization (emu/g)	0.065	0.056	0.059	0.052	0.047	0.042
Coercivity (Oe)	~198	~14	~158	~11	~130	~10

5.4 Summary

This chapter describes the role of point defects on the enhancement of ferromagnetic behaviour of vertically aligned ZnO NRs grown on Si substrates by RF magnetron sputtering technique under pure Ar atmosphere. The structural studies of the ZnO NRs from the XRD pattern reveal the high crystalline nature and hexagonal crystal structure with preferential orientation along the (002) crystallographic plane. Furthermore, it also indicates the existence of the residual compressive strain along the c-axis which is partially relaxed by the post growth treatments. Further, micro-Raman spectra provide a conclusive evidence for the partial relaxation of the compressive strain in NRs from the peak position of the non-polar phonon mode E_2^{high}. In addition, the observation of anomalous Raman modes have been attributed to the local vibrations and it corresponds to the silent modes of wurtzite ZnO. The appearance of forbidden modes illustrates the breakdown of the Raman selection rules. The role of point defects on the ferromagnetic behaviour of NRs were analyzed by optical transitions and correlated with the magnetic properties. Post growth treatment of NRs under oxygen and vacuum atmospheres significantly suppresses the point defects owing to the enhancement of the crystalline quality. The temperature dependent zero-field cooled and field cooled magnetizations reveal the coexistence of antiferromagnetism and ferromagnetism below 7 K. However, the ferromagnetism is dominant and stable between 7 K and room temperature. The decrease of ferromagnetism in NRs is directly associated with the compensation of point defects such as zinc and oxygen vacancies as substantiated by the radiative transition between shallow donor and acceptor energy levels. These results confirm that the point defects play an important role in enhancing the room temperature ferromagnetism in ZnO NRs.